

Thermal Modeling of Mars Ground for Surface Missions

Edgardo Farias[1], Matthew Redmond[2], Pradeep Bhandari[3], Jason Kempenaar[4], Keith Novak[5]
Jet Propulsion Laboratory, California Institute of Technology, Pasadena, CA, 91109

Thermal analysis packages are capable of including ground temperature effects for orbital and surface thermal analyses. In particular, Thermal Desktop® offers the option of specifying ground temperatures as a function of time for planetary surface modeling. While suitable for many cases, this approach is not sufficient if an object has local interactions with the ground that could significantly affect the ground temperature. Ground modeling is necessary for the Mars 2020 rover thermal design and analysis since shadowing and heat dissipation from the rover's Multi-Mission Radioisotope Thermoelectric Generator (MMRTG) can result in significant temperature deviations of the local ground. The Mars 2020 thermal team is explicitly modeling the Martian ground so that these local temperature effects can be captured. The upper portion of the ground is modeled, and material and optical properties of the ground are varied in order to match data collected from orbiting science instruments. Atmospheric surface temperature, sky temperatures, and solar loads from a Mars General Circulation Model (GCM) are used as boundary conditions, resulting in a ground surface temperature profile consistent with the GCM predictions. The rover model is then placed on this modeled ground so that the effects of shadowing and MMRTG dissipation on the ground temperature can be captured.

Nomenclature

abs	=	solar absorptivity
α	=	thermal diffusivity
d	=	penetration depth
c_p	=	heat capacity
ε	=	IR emissivity
GCM	=	General Circulation Model
I	=	thermal inertia
k	=	thermal conductivity
L_s	=	solar longitude
LTST	=	local true solar time
MMRTG	=	Multi-Mission Radioisotope Thermoelectric Generator
MSL	=	Mars Science Laboratory
ω	=	angular frequency
ρ	=	density
T	=	period
TES	=	Thermal Emission Spectrometer
WCC	=	Worst Case Cold
WCH	=	Worst Case Hot
WRF	=	Weather Research and Forecasting

[1] Thermal Engineer, JPL, Instrument and Payload Thermal Engineering, 4800 Oak Grove Drive, Pasadena, CA 91109, M/S 125-123.
[2] Thermal Engineer, JPL, Instrument and Payload Thermal Engineering, M/S 125-123.
[3] Principal Engineer, JPL, Propulsion, Thermal, and Materials Systems , M/S 125-123.
[4] Thermal Engineer, JPL, Instrument and Payload Thermal Engineering, M/S 125-123.
[5] Principal Engineer, JPL Spacecraft Thermal Engineering, M/S 125-123.

I. Introduction

NASA is currently developing the Mars 2020 rover which is scheduled to launch to Mars in the summer of 2020. The design for this rover is based on the design of the MSL Curiosity rover which has been operating on Mars since 2012. The Mars 2020 rover will carry with it a new suite of instruments to study the Martian landscape and environment. One of the prime objectives for this mission is to collect rock and regolith samples for potential future return to Earth. These samples will be extracted from the ground via a coring drill, stored in sealable tubes, and left on the surface. Understanding the ground temperature is important, as the ground acts a radiation surface that interacts with the rover, and knowing the temperature history of collected samples could be important during the scientific study of the collected samples. The thermal team has been working on a system-level rover thermal model to help inform in the design and operability of the rover.[1] This system level model includes an explicit model of the Mars ground so that interactions between the rover and the ground can be captured.

Modeling of the Mars environment began in the 1960s with numerical models aimed at studying the atmospheric and temperature conditions of Mars.[2] This modeling has evolved into the Mars General Circulation Model (GCM), capable of outputting ground, air, and sky temperatures at a given location on Mars. Environment predictions for the Mars 2020 mission were generated using a 1-D version of the Mars Weather Research and Forecasting GCM (MarsWRF GCM).[3,4] This model uses measured values of albedo and thermal inertia from the Thermal Emission Spectrometer (TES) onboard the Mars Global Surveyor orbiter.[5-7] The resultant temperature predictions from the model are used by the thermal team as inputs for radiation and convection boundaries. This process is similar to the approach taken by MSL to predict the temperature conditions of the landing site prior to launch.[8]

II. Worst Case Hot and Worst Case Cold Mars Environments

The Level 1 requirement for the Mars 2020 landing site latitude range is from 30° South to 30° North. A total of eight potential landing sites were selected at the end of the 2nd in a series of Landing Site Workshops (LSW) in August 2015.[9] Of the top 8 potential landing sites, the most southerly landing site will result in the most extreme environments (hottest summers and coldest winters) due to the eccentricity and obliquity of the Mars orbit. The southernmost landing site from the top 8 sites is Holden Crater, located at 26° South. The MarsWRF GCM was used to generate predicted environment conditions for Holden Crater to be used for thermal analysis. Figure 1 shows the predicted ground temperature, atmosphere temperature, sky temperature, and total (direct and diffuse) ground solar load for Holden Crater in the Worst Case Hot (WCH) summer condition, which occurs at L_s=259. Figure 2 shows the predicted ground temperature, atmosphere temperature, sky temperature, and total solar load for Holden Crater in the Worst Case Cold (WCC) winter condition, which occurs at L_s=91. Of note is that the minimum and maximum ground temperatures in WCH are -65 °C and 32 °C, respectively. For WCC the minimum and maximum ground temperatures are -103 °C and -48 °C, respectively. These temperature profiles do not take into account local interactions with any hardware on the surface.

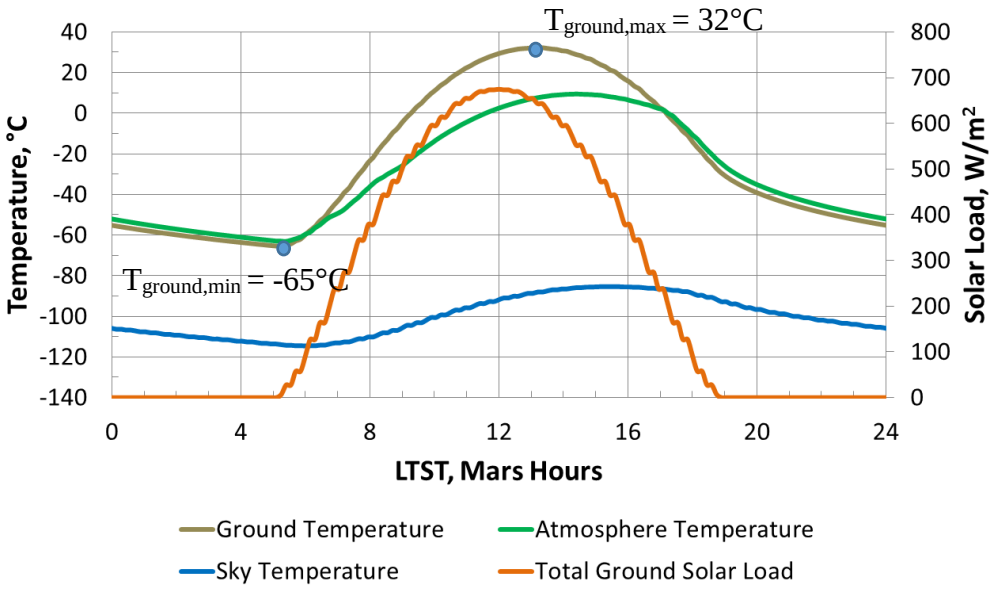

Figure 1. Holden Crater Worst Case Hot predicted environment from the Mars General Circulation Model

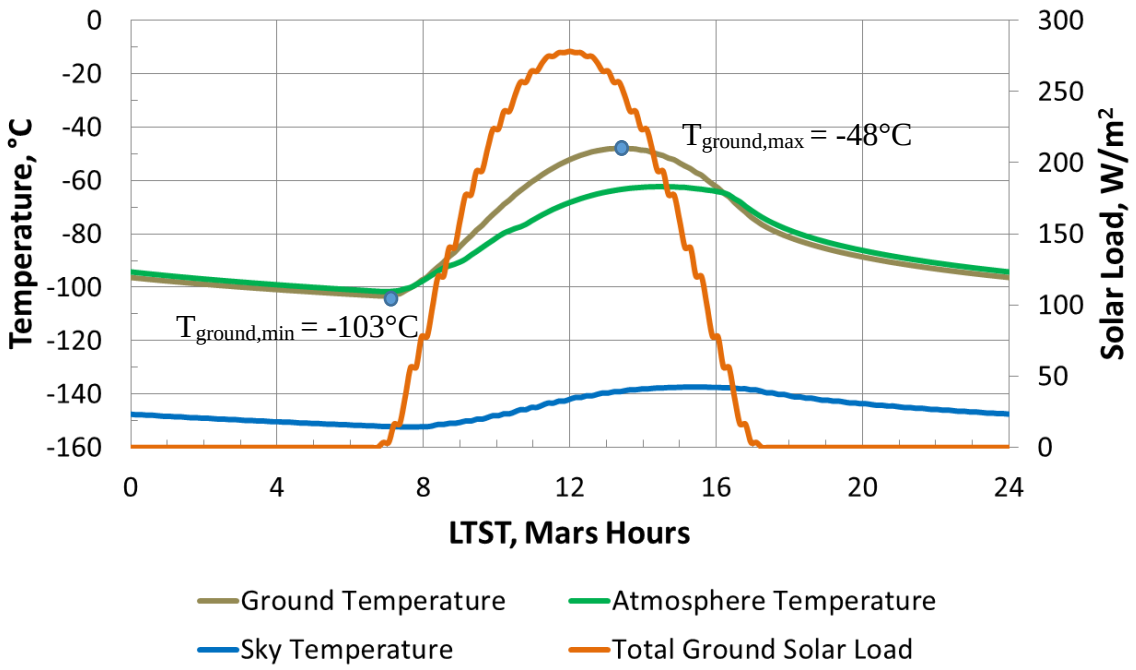

Figure 2. Holden Crater Worst Case Cold predicted environment from the Mars General Circulation Model

III. Local Ground Modeling

The goal for explicitly modeling the local ground within the rover model is to be able to capture local temperature effects that are not predicted from the GCM. The rover system thermal model and the local ground model are being made in Thermal Desktop®, a CAD-based software package for thermal modeling and analysis. This software has an orbital and planetary analysis feature. The environment data provided from the GCM is input into Thermal Desktop® as boundary temperatures. While sufficient for many surface applications, using a boundary ground temperature is not fully sufficient for the rover thermal model because shadowing and heat dissipation from the Multi-Mission Radioisotope Thermoelectric Generator (MMRTG) can significantly change local ground temperatures. However, the far field ground is modeled as a diurnally varying temperature boundary condition, in accordance with the GCM results.

Locally, a 5.4m x 4.6m section of ground is explicitly modeled so that any and all interactions with the rover can be accounted for. Figure 3 shows ground discretization into 99 lateral surface nodes. A greater node density is used near the high-dissipating MMRTG. Six ground layers were made with thicknesses of 0.1cm, 0.5cm, 2.5cm, 5cm, 12cm, and 40cm, for a total ground thickness of ~ 60 cm. The ground thermophysical and thermoptical properties are summarized in Table 1. The value of thermal inertia arises from the TES measurements data analysis. The values of density and heat capacity are assumed constant values as they do not significantly vary between different rock types, whereas thermal conductivity can vary by orders of magnitude. The value for solar absorptivity also comes from TES albedo measurements, where *abs=1-albedo*.

Table 1. Ground thermophysical and thermoptical properties used for modeling and analysis for Holden Crater landing site.

Thermal Inertia, *I*	**362 $Jm^{-2}K^{-1}s^{-1/2}$**
Thermal Conductivity, *k*	**0.1092 $Wm^{-1}K^{-1}$**
Density, ρ	**1500 kgm^{-3}**
Heat Capacity, c_p	**800 $Jkg^{-1}K^{-1}$**
Solar Absorptivity, *abs*	**0.868**
IR Emissivity, ε	**0.95**

The amount of ground thickness that needs to be explicitly modeled is a strong function of the assumed ground properties. Closed form solutions of a semi-infinite body with a sinusoidal varying wall temperature are available in literature, and do a good job of approximating sub-surface ground temperature. The penetration depth at which surface temperature amplitude is reduced to a factor of 0.01 has been given as Equation 1, and can be shown to be equivalent to Equation 2.[10] In these Equations, α is thermal diffusivity, ω is angular frequency, k is thermal conductivity, ρ is density, c_p is specific heat, and T is the sinusoidal period. Using this equation, a Martian diurnal cycle (T = 24.6 hours) with ground conductivity k=0.1092 W/m-K, density ρ = 1500 Kg/m^3, and specific heat c_p = 800 J/Kg-K results in a penetration depth of d=60 cm.

$$d = 4.61\sqrt{\frac{2\alpha}{\omega}} \tag{1}$$

$$d = 6.52\sqrt{\frac{kT}{\rho c_p}} \tag{2}$$

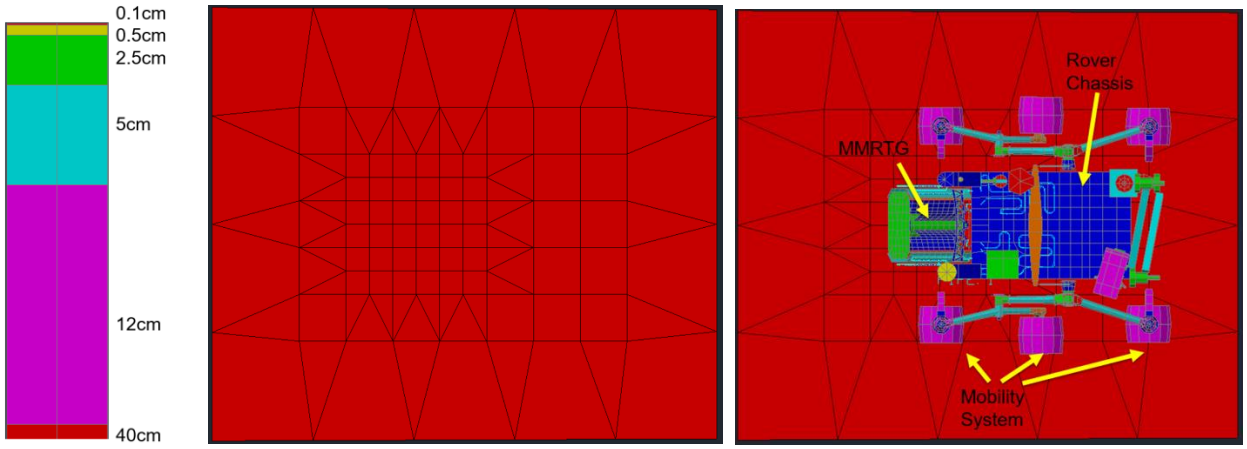

a) b) c)

Figure 3. Discretization of the ground thermal model in: a) vertical direction and b) lateral direction with c) the rover model placed above the ground. Greater node density is used in the vicinity of the MMRTG.

The ground model was first run without the rover so that model adjustments could be made. The goal was to match the surface temperature of the modeled ground with the ground temperature predicted by the GCM. The surface temperature of the modeled ground matched the predicted GCM profile fairly well using only the GCM sky temperature and solar flux. The ground temperature profile was further tuned by accounting for convection with the atmosphere boundary temperature to get a closer match to the GCM predicted temperature. A convection coefficient of 1.5W/m^2 was used for Holden WCH, and a convection coefficient of 1.0W/m^2 was used for Holden WCC. The final temperature fit of the modeled ground matched within 5 °C of the GCM temperature predictions, as shown in Figure 4. This simple ground model is therefore sufficient for use within the rover model and can be used to determine local ground effects from interactions with the rover. The MSL thermal analysis used a similar approach in local ground modeling that is presented here; however, their approach did not account for ground-ambient convection. As a result, MSL ground temperature predictions were not as accurate.

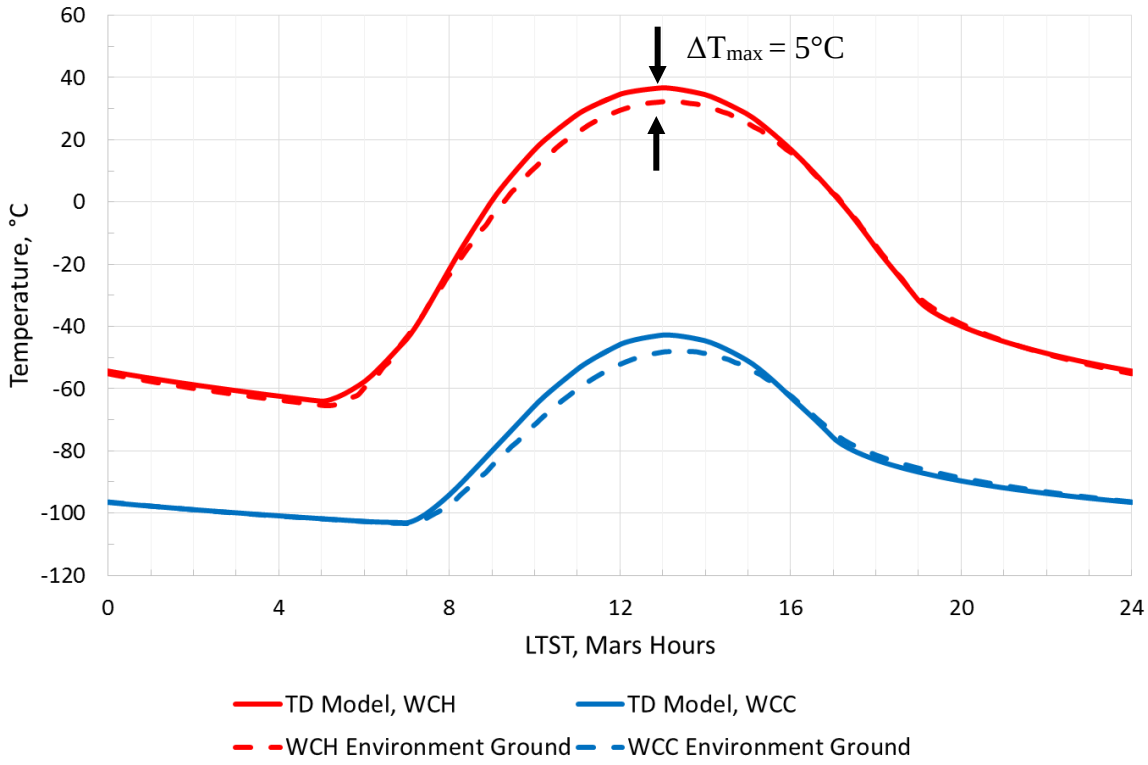

Figure 4. Thermal Desktop modeled ground temperature compared to predicted ground temperature generated by the GCM for the worst case hot and worst case cold conditions.

IV. Mars 2020 Rover Effects on Ground Temperature

The rover model is placed on top of the ground model, as shown in Figure 3, so that the effects of shadowing and MMRTG dissipation can be accounted for. Shadowing is important as the rover will block solar flux on the ground, decreasing local ground temperatures during the day. The rover also reduces the heat loss to the sky at night, resulting in increased ground temperatures at night. The ground temperature directly below the rover's belly pan is shown in Figure 5. During the daytime, the rover blocks incoming solar flux resulting in colder local ground temperatures. During the night, this portion of the ground has a reduced view to the sky, resulting in reduced heat losses and warmer ground temperatures. The effects of shadowing can further be seen in Figures 7 and 8 which show the incident environmental heat rate (W) on the ground. Local ground that is blocked by the rover experiences less solar heating.

MMRTG dissipation is also expected to have a significant effect on the local ground temperature as it can operate as hot as 200°C and dissipate up to ~ 2000W of heat. The effect of the MMRTG on ground temperature is shown in Figure 6. The ground in the vicinity of the MMRTG experiences a temperature rise throughout the day due to the heat dissipation from the MMRTG. The effects of shadowing are still present, but their effects are reduced in this area. The hottest predicted ground temperature underneath the MMRTG in this case is 56°C. Figures 9 and 10 show ground temperature contour plots for the times at which the hottest ground temperature occurs—12:00 for the Holden WCH environment and 13:00 for the Holden WCC environment. In the Holden WCH environment, there is a 78°C variation in the ground temperature as a result of MMRTG dissipation and blockage from the rover. There is a 56°C variation local ground temperature in WCC due to these effects. These large variations in temperature would not have been accounted for if the ground temperature from the GCM was applied to the local ground. The GCM ground temperature, however, is still applied to the far field ground as a boundary temperature.

A local ground model that accounts for shadowing and MMRTG dissipation results in a ~5C temperature change for several of the exterior rover componets. Though not a large effect, it is still important to incorporate local ground into the rover system model. Moreover, this type of ground modeling will be necessary where ground interactions will have a larger temperature effect, such as analysis of the samples tubes on the ground or in potential future missions to Mars.

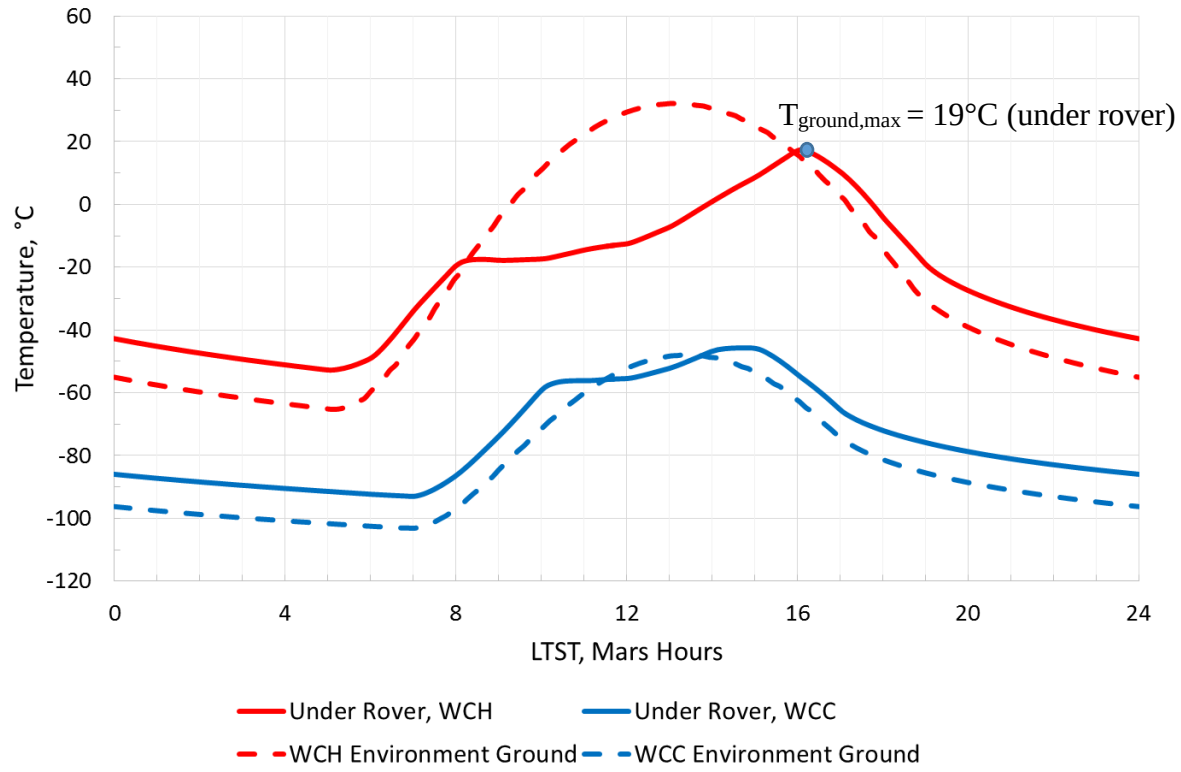

Figure 5. Effects on local ground temperature from shadowing by the rover.

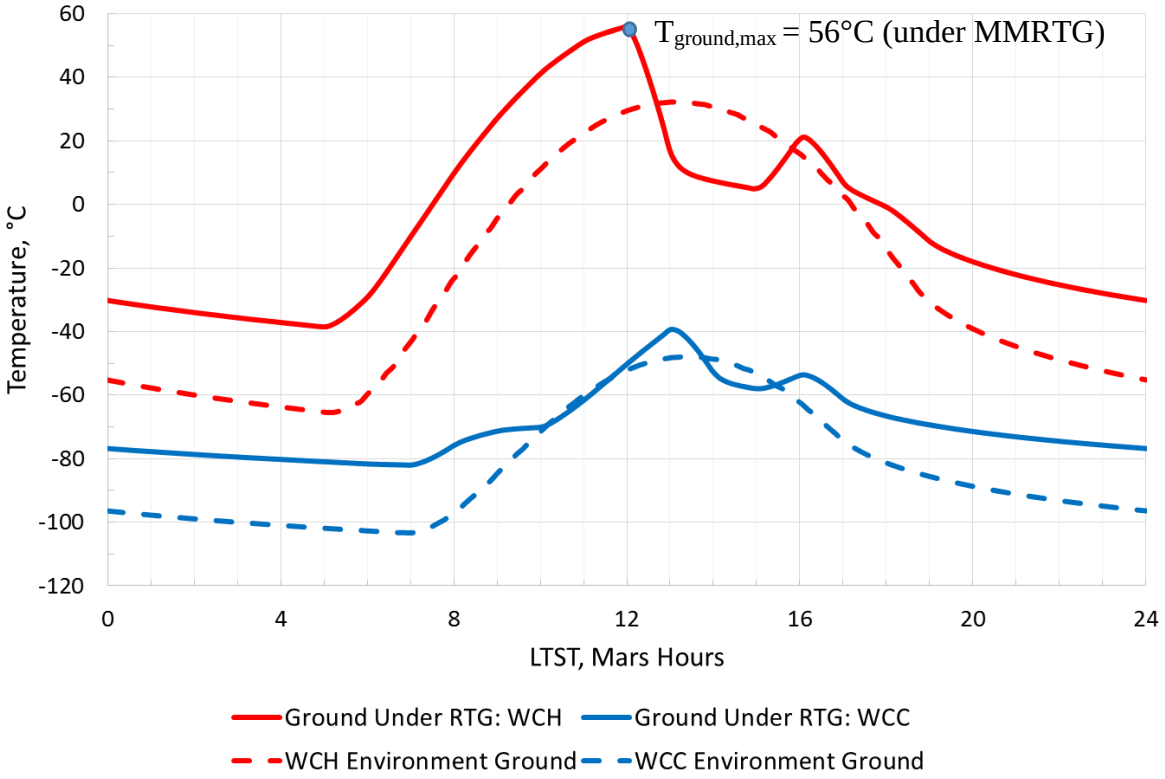

Figure 6. Effects on local ground temperature from dissipation by the rover MMRTG.

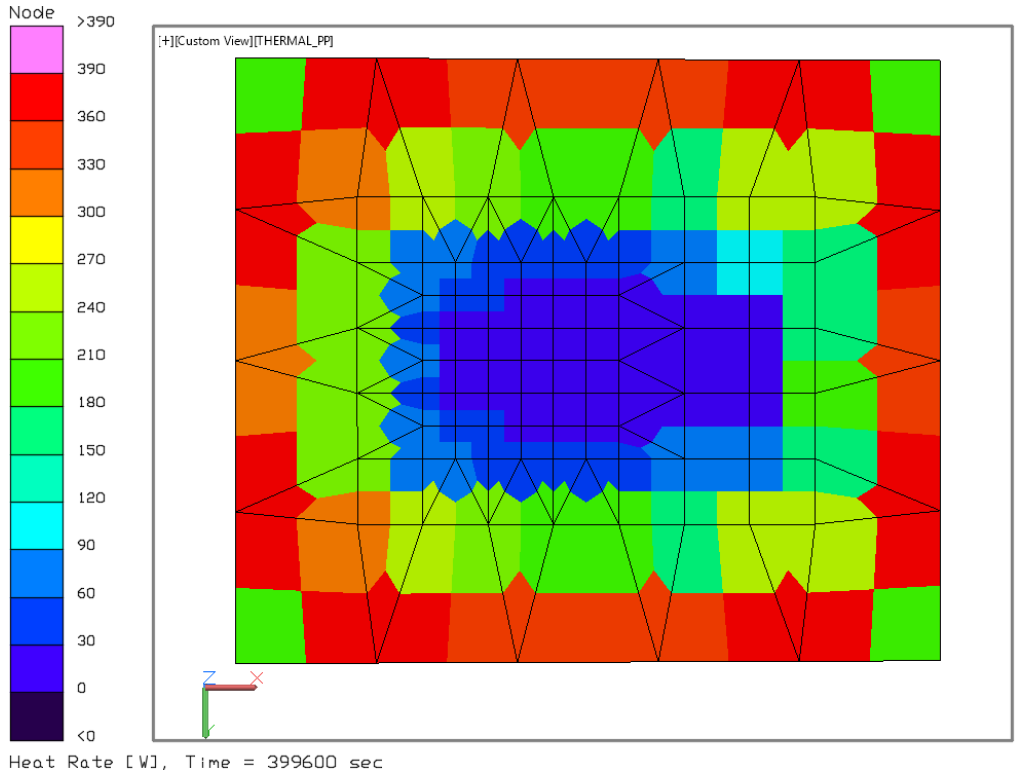

Figure 7. Incident environmental heat rate (W) on ground with rover present at time of hottest ground temperature for WCH—12:00 LTST.

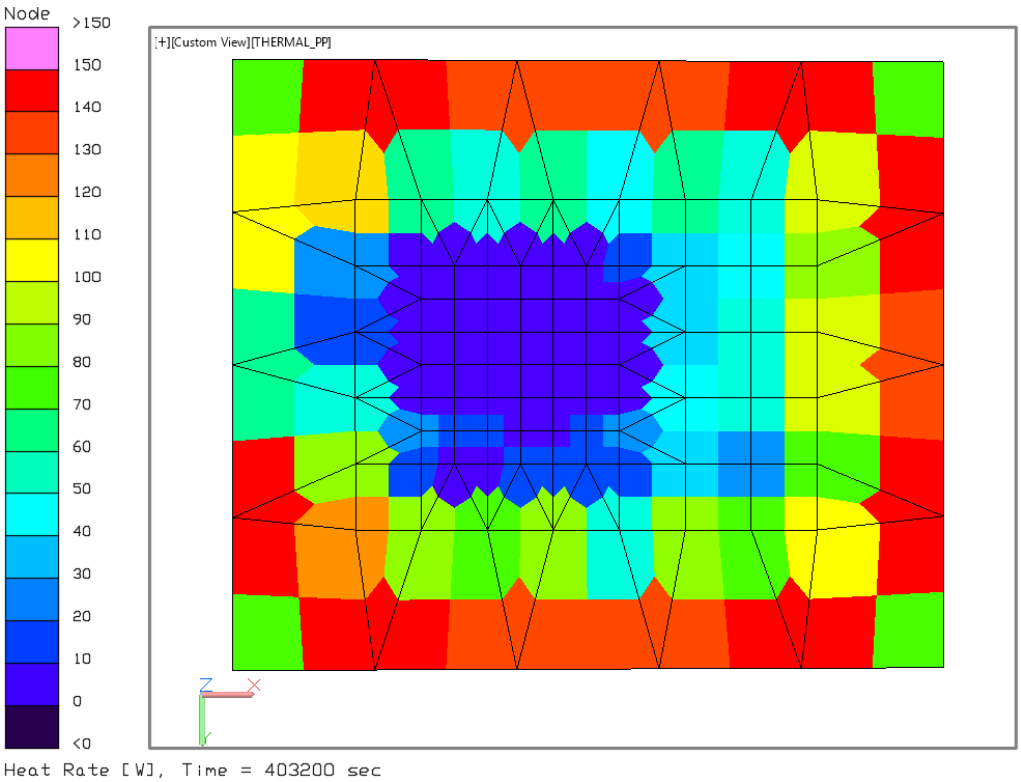

Figure 8. Incident environmental heat rate (W) on ground with rover present at time of hottest ground temperature for WCC—13:00 LTST.

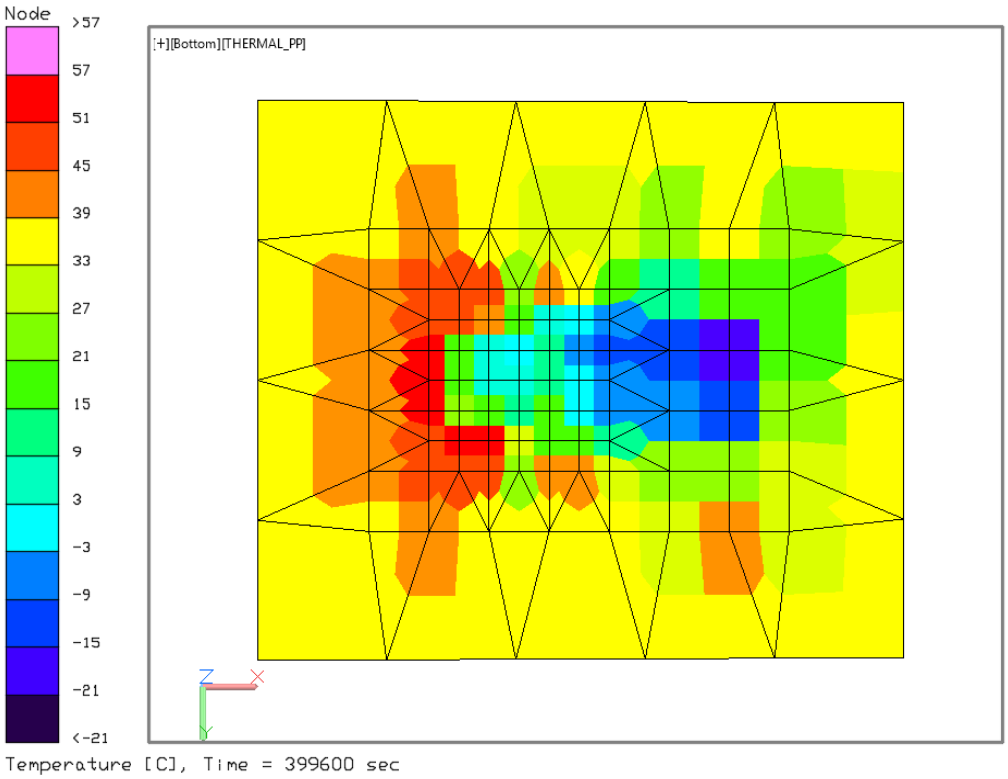

Figure 9. Ground temperature contour with rover present at time of hottest ground temperature for WCH—12:00 LTST.

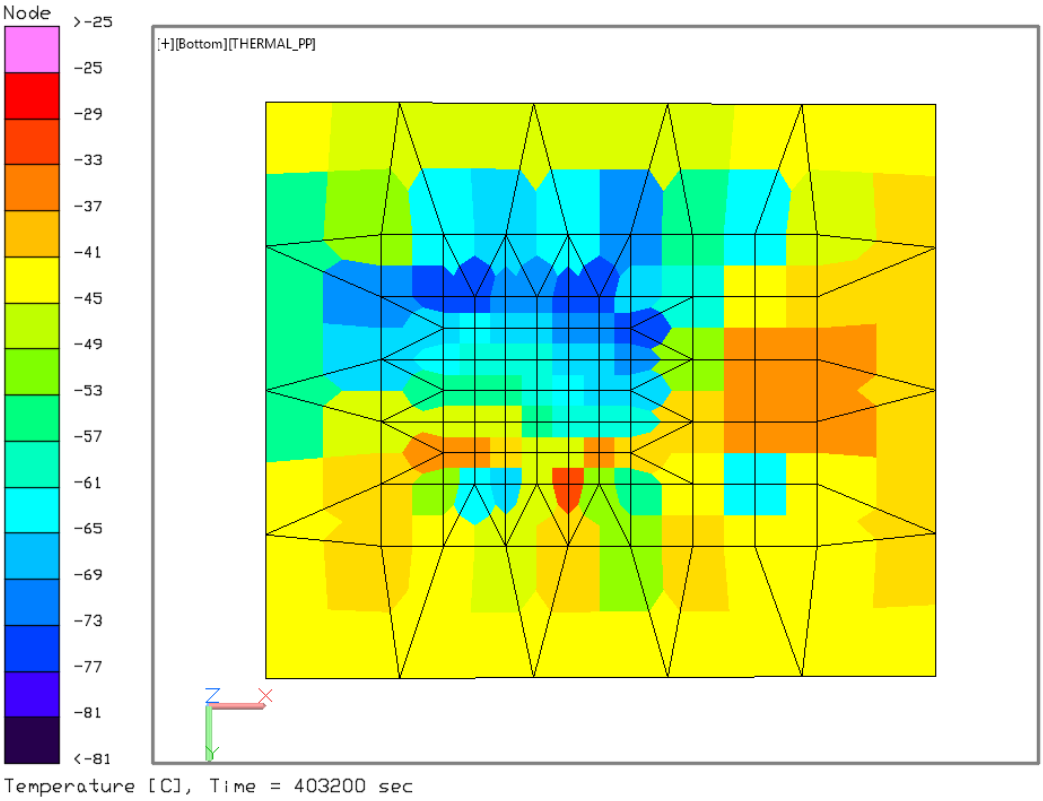

Figure 10. Ground temperature contour with rover present at time of hottest ground temperature for WCC—13:00 LTST.

V. Subsurface Ground Temperatures

One of the goals for the Mars 2020 mission is to collect and store rock and regolith samples for potential future return to Earth. The rock samples will be collected by a coring drill which has a collection tube internal to the drill bit that will capture and store the rock core sample. Collected samples are expected to be between 5 and 9 cm long, with a target length of 8 cm. Once removed from the ground by the drill, subsurface rock samples will be exposed to the Mars surface and ambient environment. The temperatures at the surface can vary significantly from the subsurface temperatures. As a result, it is desirable to understand the temperature history of the collected samples.

In this analysis, a similar ground model as the model shown in Figure 3 was used to determine ground temperatures at a depth of 8 cm and at the surface. However, in this model, the ground was modeled to a depth of 1 m, corresponding to the penetration depth of solid rock with thermal inertia, I=1550 $Jm^{-2}K^{-1}s^{-1/2}$. It should be noted that these results assume that the surface thermal properties are uniform. In reality, it is unlikely for Mars to have such uniform properties, especially for very high thermal inertias since it implies that the upper ~ 1 m of ground is solid rock.

This analysis was performed for four ground types and two environments. The ground types were: dust, loose regolith, consolidated regolith, and solid rock. Table 2 shows the assumed thermal inertia for each ground type along with the resultant thermal conductivity (density and specific heat are kept constant once again at 1500 Kg/m^3 and 800 J/Kg-K respectively). The environments used were both summer environments, a WCH 27°S GCM environment and a 15°N approximate summer environment. These are the same environments that were used in an analysis of a sample tube placed on the Martian ground.[11]

Table 2. Ground thermal inertia and thermal conductivity for varying ground types.

	Thermal Inertia, I $Jm^{-2}K^{-1}s^{-1/2}$	**Thermal Conductivity, k $Wm^{-1}K^{-1}$**	**Penetration Depth, d m**
Dust	**75**	**0.0047**	**0.121**
Loose (Sandier) Regolith	**220**	**0.04**	**0.356**
Consolidated (Rockier) Regolith	**400**	**0.1333**	**0.648**
Solid Rock	**1550**	**2.0**	**2.509**

The resulting diurnal ground temperatures at the surface and at a depth of 8 cm are shown in Figures 11 and 12 for the WCH 27°S and 15°N summer environment, respectively. It is clear that surface temperature variations are more extreme than sub-surface variations. In addition, lower thermal inertia ground types (with lower thermal conductivity) produce more extreme surface variations and less extreme sub-surface variations. Conversely, higher thermal inertia ground types (with higher thermal conductivity) produce less extreme surface variations and more extreme sub-surface variations. This makes sense since lower thermal inertia ground types have very small penetration depths (less participating mass) and higher thermal inertia ground types have large penetration depths (more participating mass).

Figure 13 gives a summary of the key results pertaining to the maximum sample temperature history. Lower thermal inertia ground types (with lower thermal conductivity) have warmer peak surface temperature histories, cooler sub-surface temperature histories, and large temperature gradients. Higher thermal inertia ground types (with higher thermal conductivity) have cooler peak surface temperature histories, cooler sub-surface temperature histories, and small temperature gradients. In addition, it is clear that the WCH 27°S environment samples have 20 to 30 °C warmer temperature histories than the 15°N summer environment at both the surface and the sub-surface. All subsurface max temperatures are lower than the corresponding surface max temperature. As a result of core sample acquisition, all subsurface samples will get exposed to temperatures that they likely have not been exposed to in many years.

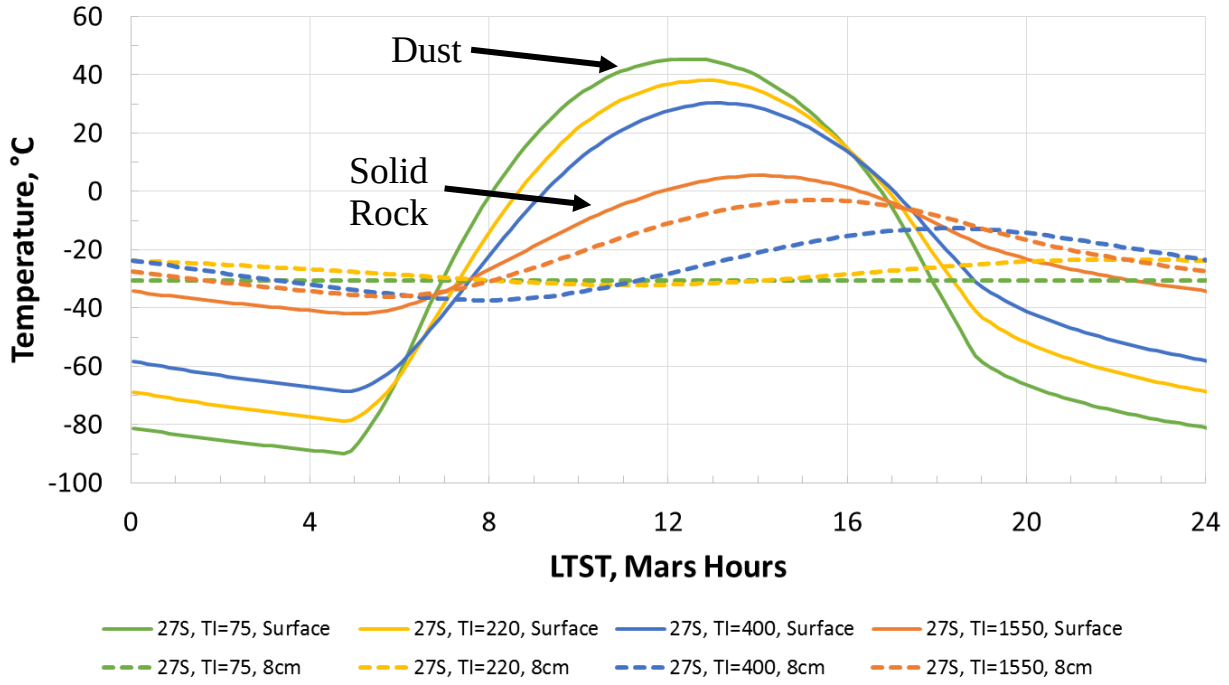

Figure 11. Predicted diurnal ground temperatures for the WCH 27°S environment at the surface and at a depth of 8 cm as a function of thermal inertia.

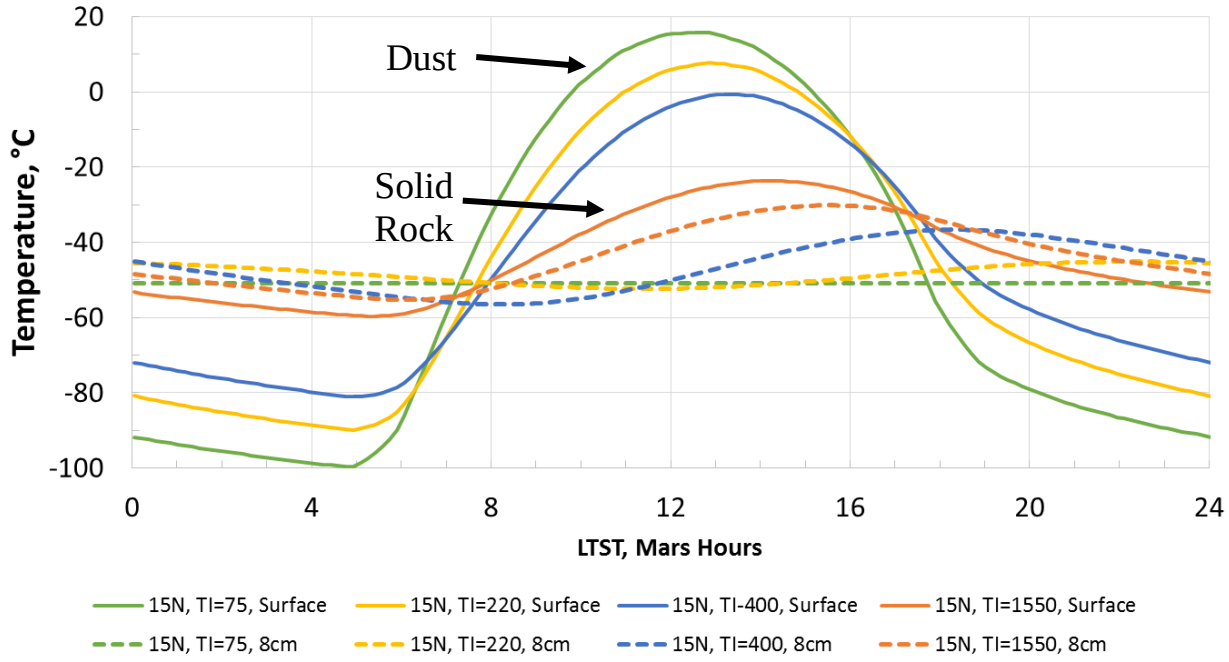

Figure 12. Predicted diurnal ground temperatures for the 15°N summer environment at the surface and at a depth of 8 cm as a function of thermal inertia.

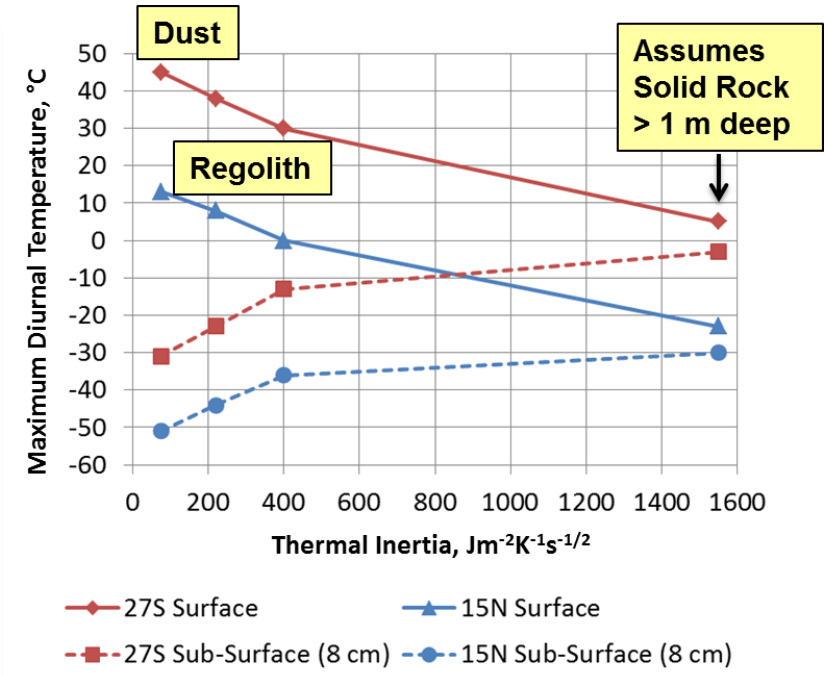

Figure 13. Max surface and subsurface ground temperatures as a function of thermal inertia (ground type) for two different Mars summer environments.

VI. Conclusion

A simple method of modeling the Mars ground has been demonstrated and shown to predict ground temperatures that match the significantly more complex Mars GCM predictions. This simple ground model is being used by the Mars 2020 thermal team to capture the effect of rover shadowing and MMRTG dissipation on the local ground temperature. These two effects together can result in up to a 78 °C variation in the local ground temperature. Modeling of local ground allows for a more accurate radiation boundary condition for the rover and ultimately allows for more accurate rover temperature predictions; the addition of local ground has a ~5C effect on several of the exterior rover components. In addition, this modeling technique has been used to estimate surface and sub-surface ground temperatures, which can inform estimates of the temperature histories of collected Mars samples. This technique is generalized, and could be used to model more complex interactions between the Martian surface and future Mars landers and rover. It also could be extended to predict local ground temperatures on Martian slopes, in large boulder fields, or possibly even in canyons or cliffs present on the surface of Mars.

Acknowledgments

This research was carried out at the Jet Propulsion Laboratory, California Institute of Technology, under a contract with the National Aeronautics and Space Administration. © 2017 California Institute of Technology. Government sponsorship acknowledged.

References

[1]Novak, K., Kempenaar, J.G., Redmond, M., Bhandari, P., "Preliminary Surface Thermal Design of the Mars 2020 Rover," *45th International Conference on Environmental Systems*, Bellevue, Washington, July 2015.

[2]Leovy, C., Mintz, Y., "Numerical Simulation of the Atmospheric Circulation and Climate of Mars," *Journal of the Atmospheric Sciences*, Vol. 26, No. 6, November 1969.

[3]Richardson, M.I., Toigo, A.D., Newman, C.E., "PlanetWRF: A general purpose, local to global numerical model for planetary atmospheric and climate dynamics," *Journal of Geophysical Research*, Vol. 112, E09001, September 2007.

[4]Toigo, A.D., Lee, C., Newman, C.E., Richardson, M.I., "The impact of resolution on the dynamics of the martian global atmosphere: Varying resolution studies with the MarsWRF GCM," *Icarus*, Vol. 221, August 2012.

[5]Putzig, N.E., Mellon, M.T., "Thermal behavior of horizontally mixed surface on Mars," *Icarus*, Vol. 191, April 2007.

[6]Putzig, N.E., Mellon, M.T., "Apparent thermal inertia and the surface heterogeneity of Mars," *Icarus*, Vol 191, June 2007.

[7]Christensen, P.R., et al, "Mars Global Surveyor Thermal Emission Spectrometer experiment: Investigation description and surface science results," *Journal of Geophysical Research*, Vol. 106, No. E10, October 2001.

[8]Vasavada, A.R., et al, "Assessment of Environments for Mars Science Laboratory Entry, Descent, and Surface Operations," *Space Science Reviews*, Vol. 170, June 2012.

[9]Farley, K., Williford, K., Grant, J., Golombek, M., Chen, A., "Letter describing the downselected sites," https://marsnext.jpl.nasa.gov

[10]Glicksman, L., Lienhard, J., *Modeling and Approximation in Heat Transfer*, Cambridge University Press, August 2016.

[11]Redmond, M., Sherman, S., Bhandari, P., and Novak, K., "Thermal Design, Analysis, and Sensitivity of a Sample Tube on the Martian Surface," *47th International Conference on Environmental Systems*, Charleston, South Carolina, July 2017.